

---

This is the **accepted version** of the journal article:

Xu, Nuohan; Kang, Jian; Ye, Yangqing; [et al.]. «Machine learning predicts ecological risks of nanoparticles to soil microbial communities». *Environmental Pollution*, Vol. 307 (August 2022), art. 119528. DOI 10.1016/j.envpol.2022.119528

---

This version is available at <https://ddd.uab.cat/record/309269>

under the terms of the  license

1 **Machine learning predicts ecological risks of nanoparticles to soil microbial**  
2 **communities**

3 Nuohan Xu<sup>1</sup>, Jian Kang<sup>1</sup>, Yangqing Ye<sup>2</sup>, Qi Zhang<sup>1</sup>, Mingjing Ke<sup>1</sup>, Yufei Wang<sup>3</sup>,  
4 Zhenyan Zhang<sup>1</sup>, Tao Lu<sup>1</sup>, W.J.G.M. Peijnenburg<sup>4,5</sup>, Josep Penuelas<sup>6,7</sup>, Guanjun Bao<sup>2</sup>,  
5 \*, Haifeng Qian<sup>1,\*</sup>

6

7 1. College of Environment, Zhejiang University of Technology, Hangzhou, Zhejiang  
8 310032, P. R. of China

9 2. College of Mechanical Engineering, Zhejiang University of Technology, Hangzhou,  
10 Zhejiang 310032, P. R. of China

11 3. Tongji Medical College, Huazhong University of Science and Technology, Wuhan,  
12 Hubei 430030, P. R. of China

13 4. Institute of Environmental Sciences (CML), Leiden University, RA Leiden 2300,  
14 the Netherlands

15 5. National Institute of Public Health and the Environment (RIVM), Center for Safety  
16 of Substances and Products, P.O. Box 1, Bilthoven, the Netherlands

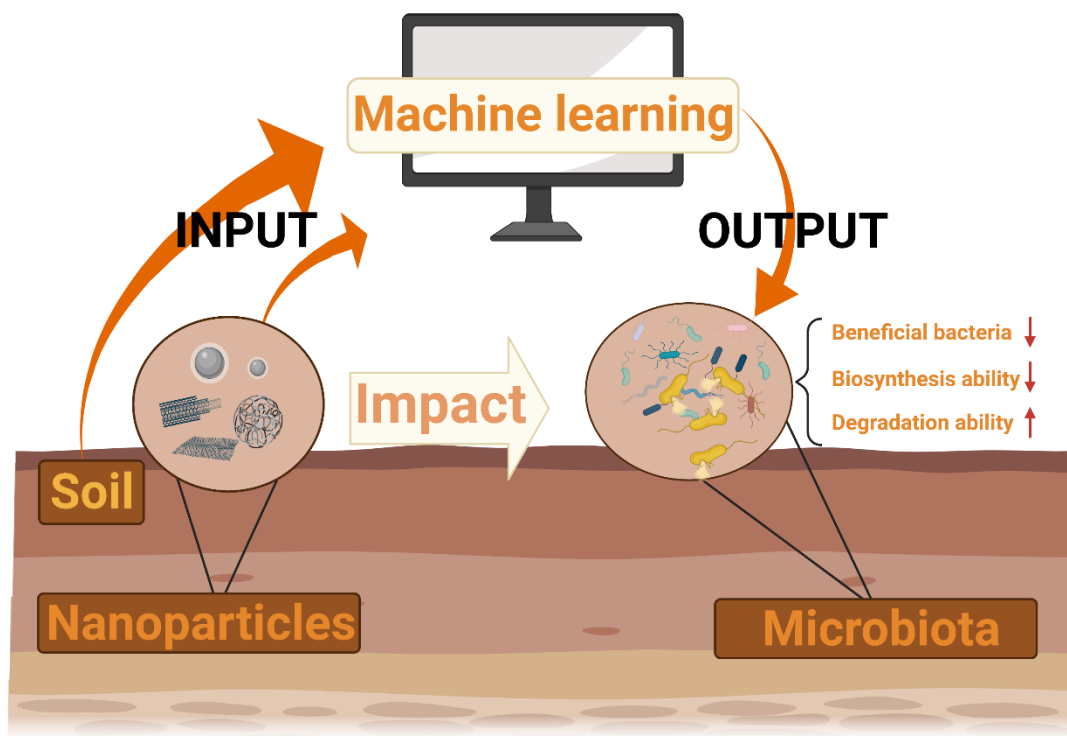
17 6. CSIC, Global Ecology Unit CREAM- CSIC-UAB, Bellaterra, Barcelona 08193,  
18 Catalonia, Spain.

19 7. CREAM, Campus Universitat Autònoma de Barcelona, Cerdanyola del Vallès,  
20 Barcelona 08193, Catalonia, Spain.

21

---

\* Correspondence Author: E-mail: [gjbao@zjut.edu.cn](mailto:gjbao@zjut.edu.cn) (Bao G.); E-mail: [hfqian@zjut.edu.cn](mailto:hfqian@zjut.edu.cn) (Qian H.).



25 **Abstract**

26 With the rapid development of nanotechnology in agriculture, there is increasing  
27 urgency to assess the impacts of nanoparticles (NPs) on the soil environment. This  
28 study merged raw high-throughput sequencing (HTS) data sets generated from 365  
29 soil samples to reveal the potential ecological effects of NPs on soil microbial  
30 communities by means of metadata analysis and machine learning methods. Metadata  
31 analysis showed that treatment with nanoparticles did not have a significant impact on  
32 the alpha diversity of the microbial community, but significantly altered the beta  
33 diversity. Unfortunately, the abundance of several beneficial bacteria, such as *Dyella*,  
34 *Methylophilus*, *Streptomyces*, which promote the growth of soil protozoa and plants,  
35 and improve pathogenic resistance, was reduced under the addition of synthetic  
36 nanoparticles. Furthermore, metadata demonstrated that nanoparticles treatment  
37 weakened the biosynthesis ability of cofactors, carriers, and vitamins, and enhanced  
38 the degradation ability of aromatic compounds, amino acids, etc. This is unfavorable  
39 for the performance of soil functions. Besides the soil heterogeneity, machine learning  
40 uncovered that a) the exposure time of nanoparticles was the most important factor to  
41 reshape the soil microbial community, and b) long-term exposure decreased the  
42 diversity of microbial communities and the abundance of beneficial bacteria. This  
43 study is the first to use a machine learning model and metadata analysis to investigate  
44 the relationship between the properties of nanoparticles and the hazards to the soil  
45 microbial community from a macro perspective. This guides the rational use of  
46 nanoparticles for which the impacts on soil microbiota are minimized.

47 **Keywords:** Machine learning; Soil ecosystems; Microbiota; Nanoparticles; Metadata

48 analysis; Ecotoxicity.

49

## 50 **1. Introduction**

51 Nanoparticles (NPs) are becoming extensively used additives in modern intensive  
52 agriculture. They are widely used in various applications, including the improvement  
53 of the quality of saline-alkali soil (Guerriero et al., 2021), the maintenance of  
54 vegetables fresh (Fayaz et al., 2009), and the design of new agricultural  
55 nanopesticides (You et al., 2018). The unintended release of NPs may though lead to  
56 their accumulation in soil and pose potential ecological and human health risks (Peng  
57 et al., 2017). The production of NPs in the USA was estimated to be 2.8 to 20 tons per  
58 year in 2011 and will reach 2.5 million tons per year by 2025 (Hendren et al., 2011;  
59 McShane et al., 2012), and the soil is considered to be the sink of these NPs (Sun et  
60 al., 2015). Soil bacteria helps crops grow by improving soil structure, and recycling of  
61 soil nutrients (Bahram et al., 2018; Guo et al., 2020; Qu et al., 2020; Ray et al., 2020).  
62 Therefore, the stability of soil microbial communities is one of the key factors in the  
63 maintenance of the soil ecosystem function (Delgado-Baquerizo et al., 2016). For  
64 example, altered microbial communities will interfere with the biosynthesis of  
65 nutrients from the soil pool and the degradation of organic matter into inorganic  
66 matter (Lehmann et al., 2017).

67 The negative influence of NPs on soil microbiota is related to the composition,  
68 concentration, type, exposure time, and particle size of NPs (Zhang et al., 2020b).

69 NPs have detrimental effects on microbial activity, abundance, and diversity (Simonin  
70 and Richaume, 2015) and alter ecosystem functioning (Simonin et al., 2018). The  
71 microbiota of soils submitted to NPs treatments have been characterized by using

72 high-throughput sequencing (HTS) methods that show that microbial communities are  
73 redrawing the map of the microbial kingdom by altering its enormous - and largely  
74 uncharted - taxonomic and functional diversity (Nilsson et al., 2019). Development of  
75 HTS methods help to reveal the effects of NPs on the structure and stability of the soil  
76 microbial community (Zhang et al., 2020a). Open-access HTS data from independent  
77 studies and the development of analytical workflows provide a new opportunity to  
78 evaluate global microbial patterns (Ramirez et al., 2018; Wright et al., 2020).

79 However, independent studies have occasionally reported contrasting results due to  
80 the high heterogeneity of soils from different localities, NPs properties, and variable  
81 experimental conditions, which result in a lack of a consensus concerning microbiota  
82 responses to NPs treatment (Ben-Moshe et al., 2013; Fan et al., 2018; Zhang et al.,  
83 2018). To shed light into these responses, machine learning, can become a key tool for  
84 NPs properties identification (Wright et al., 2020; Yuan et al., 2020, Ban et al.,  
85 2020; Ahneman et al., 2018; Oh et al., 2016). In fact, machine learning combined with  
86 HTS metadata analysis have already been applied to analyze the characteristics of the  
87 soil microbiome and predicting the occurrence of *Fusarium* wilt (Yuan et al., 2020).

88 With the aim of identifying the main factors associated with the ecological impact of  
89 NPs overcoming the high heterogeneity of data in independent experiments, we  
90 integrated the available raw HTS sequences data for microbiome nanotoxicology and  
91 re-analyzed the data using machine learning. Our aims were to: (1) identify the  
92 common effects of NP treatment on soil microbial community diversity, composition  
93 and function; (2) determine how NPs affect the change in the accumulation of the

94 significant beneficial bacteria and pathogenic bacteria in soils; and (3) build a  
95 predictive model to correlate NPs properties with the stability of soil microbial  
96 communities. Accurately predicting the contribution of NP characteristics on soil and  
97 agricultural ecosystem variation can guide the wide use of eco-friendly NPs.

98

## 99 **2. Material and methods**

### 100 *2.1. Data collection and description*

101 The data of microbial high-throughput sequencing (HTS) in NPs treated and untreated  
102 soils were collected by searching the keywords “NPs and soil microbial”, “NPs and  
103 soil HTS”, “nanomaterials and soil bacterial” in Google Scholar and the National  
104 Center for Biotechnology Information (NCBI) SRA database. After filtering the  
105 sources of metadata that did not contain basic information, we grouped the data into  
106 the categories of nano-treated or -untreated soils. Since the bioproject accession  
107 numbers of the HTS data results of most microbial community studies were not  
108 uploaded, we collected approximately 63 studies matching the keywords, of which  
109 only 18 data sets could be downloaded from public databases (Table S1). We obtained  
110 632 microbial HTS samples from 10 countries around the globe (Fig. 1). After  
111 removing samples of incomplete, low-abundance sequences, and containing  
112 chlorophyll and mitochondria, and then rarefied according to the minimum frequency,  
113 there were 365 high quality bacterial samples left. Based on the data preprocessing  
114 presented above, we acquired 13 independent studies with 125 controls and 240 NPs-  
115 treated samples. The metadata were classified as from “nano-treated” and “nano-



116 untreated” after carefully read the full texts of each paper. We defined nano-treated  
117 group as the soil exposed by NPs, and nano-untreated group as the soil without the  
118 NPs treatment.

119

## 120 *2.2. Data Processing*

121 For each independent study, the HTS data were processed using QIIME2 (Version  
122 2020.8) core distribution, following the standard workflows (Bolyen et al., 2019).

123 Raw data from each of the studies were imported into QIIME2, and adaptor and  
124 primer sequences were then removed from the reads using Cutadapt (Martin, 2011).

125 The latter step was omitted for samples where the sequences had already been  
126 removed. Then, we used Dada2 to join paired end reads, denoising sequences as well  
127 as resolving amplicon sequence variants (ASVs) under default quality thresholds  
128 (Callahan et al., 2016). Dada2 was run using trim lengths determined by the read  
129 quality for each study. The samples with low reverse read qualities, which caused too  
130 few reads remaining after running Dada2, were only used the forward reads to gain  
131 more reads after Dada2. Feature tables and the representative sequence of ASVs were  
132 acquired, and then merged by the QIIME2’s merge plugin. All feature sequences were  
133 annotated with the SILVA v138 database of full-length 16S rRNA gene sequences for  
134 subsequent analysis. The workflow of this study is shown in Fig. S1. To eliminate  
135 PCR primer deviation and over amplification, we filtered the ASVs table according to  
136 the following rules: (1) the samples were rarefied to 2000 reads, and those with <2000  
137 reads were removed; (2) sequences annotated to mitochondria and chloroplasts or that

138 could not be classified at the kingdom level were removed; and (3) ASVs with a  
139 maximum number of 20 reads (1% total reads in each sample) were removed. Feature  
140 tables for each taxonomic level were then generated, and the data were converted to  
141 relative abundance.

### 142 *2.3. PICRUSt2 for prediction of metagenome functions*

143 Phylogenetic Investigation of Communities by Reconstruction of Unobserved States  
144 (PICRUSt2) is a software package suited for predicting functional abundances based  
145 on marker gene sequences (Douglas et al., 2020). Function prediction on the merged  
146 ASVs table and sequences was applied. The annotation and classification of the  
147 functional pathways were acquired through the database MetaCyc  
148 (<https://metacyc.org>) (Caspi et al., 2020).

149

### 150 *2.4. Construction of a predictive random forest model*

151 We developed a regression model established by the random forest (RF) algorithm.  
152 The established RF model not only took the properties related to NPs as independent  
153 variables, but also the properties related to the soil, with a total of 21 input variables  
154 (Table. S2). The dependent variables of the RF model were the values of Richness and  
155 Shannon of the soil microbial community previously analyzed. To ensure the  
156 prediction accuracy and applicability, we utilized the 10-fold cross validation method,  
157  $R^2$  (coefficient) and RMSE (root mean square error) to evaluate the model  
158 performance.

159 The imported dataset was partitioned into 10 folds, in which 70% of the training data

160 were used to build the regression model, and the remaining 30 % were used for  
161 prediction using the trained model. Ten-fold cross-validation with five repeats was  
162 used to verify the regression models, and we selected the model with the highest  $R^2$   
163 value for subsequent analysis. To estimate the importance of the different properties,  
164 the increase of node purity of each model was calculated by the R package  
165 ‘RandomForest’. The construction and prediction performance of the random forest  
166 regression model (n\_estimators=150, max\_leaf\_nodes=10) and the verification of the  
167 10-fold cross-validation method were both used by the scikit-learn (Version 0.24.0)  
168 library of the python language (Python 3.9).

### 169 *2.5. Statistical methods*

170 The alpha diversity index of Shannon and Richness were calculated using the R vegan  
171 and picante package (version 4.0.3). Principal co-ordinates analysis (PCoA) plots  
172 were generated from the Bray-Curtis distance created using the R package ggplot2  
173 and vegan (version 4.0.3). Permutational multivariate analysis of variance  
174 (PERMANOVA) (ADONIS, transformed data by Bray-Curtis, permutation = 999)  
175 was used to determine if beta diversity differed between NPs treated and untreated  
176 groups. A hierarchical bubble chart, sunburst chart and world map were drawn by R  
177 package ggplot2, ggmap, ggraph and igraph (version 4.0.3). Opportunistic human  
178 pathogens were searched from an online database ([https://www.bode-science-  
179 center.com/center/relevant-pathogens-from-a-z.html](https://www.bode-science-center.com/center/relevant-pathogens-from-a-z.html)). All bar charts were designed by  
180 the software Prism 5.0. The graphical abstract was created with BioRender.com. The  
181 remaining results are presented as the means  $\pm$  standard deviations (SDs). Significant

182 differences ( $p < 0.05$ ) were evaluated by Kruskal-Wallis test using the R function  
183 `kruskal.test` (version 4.0.3).

184

### 185 **3. Results**

#### 186 *3.1. Diversity and taxonomic difference after NPs treatment*

187 Alpha diversity indices (Richness and Shannon) were not significantly different  
188 between the NPs-treated and NPs-free soils (Fig. 2a), while principal coordinates  
189 analysis (PCoA) of Bray–Curtis dissimilarity with multivariate permutational analysis  
190 of variance (PERMANOVA) revealed that the structure of the microbial communities  
191 significantly differed (Fig. 2b,  $R^2 = 0.010$ ,  $p < 0.001$ ; ADONIS). At the phylum level,  
192 the soil microbial communities in all samples were mainly composed of  
193 *Proteobacteria*, *Actinobacteriota*, *Bacteroidetes*, *Acidobacteriota* etc. (Fig. 2c).

194 Among these phyla, *Proteobacteria* in NPs treatment increased significantly by 29%,  
195 while *Acidobacteriota*, *Verrucomicrobiota*, and *Planctomycetota* decreased by 31, 60,  
196 and 43%, respectively (Fig. S2). The Venn diagram illustrated that the microbial  
197 community composition of the control and NPs-treated groups shared most of the  
198 bacterial taxa, with more unique bacterial taxa in the NPs-treated group (219) than in  
199 the untreated group (114) (Fig. 2d). In conclusion, our results indicated that NPs  
200 treatment altered the microbial community composition and structure.

201

#### 202 *3.2. The profile of beneficial and pathogenic soil bacteria after NPs treatment*

203 We retrieved 33 plant growth-promoting and soil disease suppression bacteria, as well

204 as 26 pathogenic bacteria related to human and soil-borne bacteria pathogens. NPs  
205 treatment . decreased the abundances of *Methylophilus*, *Dyella* and *Streptomyces*,  
206 which are bacteria that promote plant growth, and increased the abundance of  
207 symbiotic *Burkholderia-Caballeronia-Paraburkholderia* (Fig. 3a-d). NPs treatment  
208 also increased the abundance of one pathogenic bacterium, *Sphingomonas*, (Fig.  
209 3e).

210

### 211 3.3. Functional traits of bacteria after NPs treatment

212 Most functional pathways were shared between the NPs-treated and untreated groups,  
213 but 189 out of a total of 415 functional pathways were different between the two  
214 groups (Fig. S3, Table. S3). These 189 significantly different functional pathways  
215 belong to four major categories: Biosynthesis, Degradation, Macromolecule  
216 modification, Generation of precursor metabolites and energy (Fig. 4), and 91 of them  
217 were down-regulated, whereas 98 pathways were up-regulated in the NPs treatment.  
218 In the superclass Biosynthesis, although there were a few up-regulated functional  
219 pathways, especially in Cofactor, Carrier, and Vitamin Biosynthesis, most functional  
220 pathways were down-regulated. On the other hand, most pathways in the superclass  
221 Degradation were up-regulated, such as the subclasses Aromatic Compound  
222 Degradation, Amino Acid Degradation, Carboxylate Degradation, Amine and  
223 Polyamine Degradation (Fig. 4).

224

### 225 3.4. Development of models to connect NPs characteristics and microbial community

226 *traits*

227 The models for the 10-fold cross validation displayed a robust performance  
228 (consistently high  $R^2$ , mostly > 70%) with values of  $R^2$  mostly ranging between 69  
229 and 91% (Fig. 5a) revealing a proper prediction of the microbial diversity (Fig. S4).  
230 Based on the models constructed, we analyzed the importance of each of the  
231 characteristics of the models. Regardless of whether it was the model for predicting  
232 Richness or the model for predicting the value of the Shannon index, the most  
233 important traits were related to heterogeneous soil characteristics, such as longitude,  
234 soil sampling depth, and amplification area (Fig. 5b, c). Despite heterogeneities, the  
235 exposure time of the NPs had the greatest impact on the soil microbial communities,  
236 followed by the extent of aggregation of the NPs (Fig. 5b, c). To explore the specific  
237 variation of the most important NPs property, we carried out a two-dimensional  
238 scatter diagram analysis of the NPs exposure time and the value of the Richness and  
239 Shannon indices of the microbial community. No matter the exposure time, the  
240 Richness of the microbial community decreased after NPs treatment (Fig. 5d). We  
241 separated exposure time into three phases, with the acute group treated for no more  
242 than three days, the subacute group treated in between three to 90 days, and the  
243 chronic group treated for more than 90 days. We found that acute NPs treatment  
244 increased the Shannon value, but subacute and chronic exposure decreased the  
245 Shannon value (Fig. 5d). Three beneficial bacteria were all down-regulated  
246 significantly after NPs treatment, including *Dyella*, *Methylophilus*, and *Streptomyces*.  
247 (Fig. 5e). The abundance of *Burkholderia-Caballeronia-Paraburkholderia* increased

248 after long-term exposure (Fig. 5e). However, the abundance of the human pathogen  
249 *Sphingomonas* increased under both subacute and chronic exposure conditions (Fig.  
250 5e).

251

#### 252 **4. Discussion**

253 We merged and normalized the HTS data sets of independent experiments to avoid the  
254 deviation of heterogeneous factors in traditional experiments such as sequencing  
255 depth, primers, and amplification area, and analyzed the soil microbial characteristics  
256 and potential functional features to figure out clearly and uniformly the impact of NPs  
257 on soil microbial community diversity, composition, and functions. The results of this  
258 analysis show that the treatment of NPs can cause a decrease in biomass and reduce  
259 bacterial diversity (Chen et al., 2019; Cocozza et al., 2019). This finding is consistent  
260 with previous results (Fig. 2a, 2b and 2c). *Proteobacteria*, *Acidobacteriota*,  
261 *Verrucomicrobia*, and *Planctomycetota* were four dominant bacterial phyla in soil  
262 (Yang et al., 2019). NPs treatment enriched *Proteobacteria*, including many genera of  
263 pathogenic bacteria in this phylum (Shin et al., 2015). Several beneficial soil phyla  
264 were down-regulated after NPs treatment, such as *Acidobacteriota*, which is a driver  
265 of various ecosystem processes, *Verrucomicrobia*, which is one of the most  
266 indispensable phyla that affect soil multifunctional resistance in the soil microbial  
267 community, and *Planctomycetota*, which plays an important role in global carbon and  
268 nitrogen cycles (Kielak et al., 2010; Wiegand et al., 2018; Yang et al., 2021). The  
269 decrease of beneficial bacterial genera of *Dyella*, *Methylophilus*, *Streptomyces* could

270 decrease resistance of plants to pathogenic microbiota, and weaken exogenous  
271 pollutants degradation in soil (Ali et al., 2021; Tapia-García et al., 2020; You et al.,  
272 2021). Therefore, these negative effects of NPs contamination on soil-borne beneficial  
273 bacteria aggravated potential risks to soil ecosystemic health, and the increase in the  
274 abundance of human pathogenic bacteria increased the potential risk for human health  
275 (Fang et al., 2018).

276 The soil microbiota is a crucial driver of global nutrient cycles and of plant growth  
277 regulation (Bahram et al., 2018; Finkel et al., 2020). Accurate functional prediction  
278 from our merged metadata sets by the PICRUST2 software showed that degradation  
279 pathways in NPs treatment were generally up-regulated, while several biosynthetic  
280 pathways were generally down-regulated (Fig. 4). This implies that the ability of the  
281 soil microbiota to synthesize antibiotics, siderophores, and hormones related to plant  
282 growth, was in all cases weakened (Hibbing et al., 2010). Soil microbiota submitted to  
283 NPs treatment increased the degradation of organic nutrients enhancing the tolerance  
284 to contamination (Kusi et al., 2020).

285 A complex set of data was used to obtain meaningful and regular patterns and predict  
286 various biological responses through machine learning (Ahneman et al., 2018). The  
287 non-linear regression models obtained by applying a Random Forest (RF) algorithm  
288 were built to reveal the nano-characteristics that contributed most to variations in the  
289 diversity of the soil microbial community. Compared with logistic regression, support  
290 vector machines, and other machine learning algorithms, the RF model displayed  
291 robust predictive performance for discrete as well as continuous data (Yuan et al.,



292 2020). The RF model provided the possibility to explore the most important  
293 properties of NPs that alter the stability of soil microbial community. Our developed  
294 RF models had good predictive performance with high  $R^2$  (mostly >70%). From these  
295 public data, we determined that the geographic location of the sampling site, soil type,  
296 soil acidity and alkalinity, and other heterogeneous characteristics of the soil  
297 microbiota, have greater impact on soil microbial diversity than NPs properties  
298 themselves. Notably, after removing other soil heterogeneity factors, the exposure  
299 time of NPs was the most crucial for the Richness and Shannon models we  
300 constructed, implicating that NPs displayed long-term impacts on soil microbiota  
301 (Moll et al., 2017). Although in many independent experimental kinds of research, the  
302 concentration and type of NPs were considered to be non-negligible traits affecting  
303 soil microbial communities, the profile of NPs properties by machine learning  
304 provides a baseline for using eco-friendly NPs. The potential adverse effects of NPs to  
305 the soil ecosystem can be minimized by adjusting and restricting the exposure time of  
306 NPs in soil. With the available heterogeneous data in hand, the RF model can be  
307 applied to explore unknown and complex relationships hidden in various quantitative  
308 and qualitative factors (Yu et al., 2021). However, the innovative exploration of  
309 metadata analysis combined with machine learning still has certain limitations. Due to  
310 the lack of standardization workflow of the uploaded HTS data sets, and some low-  
311 quality data sets, only 365 samples were available to construct RF models in this  
312 study. Although our models displayed good performance, they had certain limitations  
313 in explaining the impacts of NPs properties on the diversity and community of the soil

314 microbiota.

315

## 316 **5. Conclusions**

317 Ours results indicate that NPs exposure altered the structure of the soil microbial  
318 community in the studies included in this modelling exercise. The decrease of the  
319 abundance of bacteria beneficial to soil protozoa and plants increases the risk of  
320 diseases of animals and plants in the soil. NPs treatment weakens the biosynthesis  
321 ability and strengthens the degradation ability of soil microbiota, thus affecting of soil  
322 ecosystemic functioning. Long-term NPs exposure down regulated the diversity of  
323 microbial communities and the abundance of beneficial bacteria. This study provided  
324 an accurate predictive model to reveal the properties of NPs that determine soil  
325 microbial diversity and soil microbial functioning. The model provides guidance for  
326 the application of NPs in industrial, agricultural, manufacturing, and other fields to  
327 minimize environmental risks.

328

## 329 **Author contributions**

330 NX, GB, and HQ conceived the study, JK, MK and ZZ collected the data, NX, YY  
331 and TL analyzed the data, NX, QZ, YW, WP, JP and HQ wrote the manuscript.

332

## 333 **Declaration of competing interest**

334 The authors declare that they have no known competing financial interests or personal  
335 relationships that could have appeared to influence the work reported in this paper.

336

### 337 **Acknowledgments**

338 This work was financially supported by the National Natural Science Foundation of  
339 China (21976161, 21777144, and 41907210).

340

### 341 **Data availability**

342 Information for all metadata used was provided in Table S1. Raw data can also be  
343 provided by the corresponding author upon request. Codes associated with this study  
344 will be publicly available in (<https://github.com/Plantxnh/Nanoparticles>) upon  
345 manuscript acceptance.

346

### 347 **Supporting Information**

#### 348 **Tables**

349 **Table S1.** The profile of the data collected.

350 **Table S2.** The profile of feature variables of machine learning models.

351 **Table S3.** The profile of shared differential functional pathways after NPs treatment.

#### 352 **Figures**

353 **Figure S1.** Schematic of the bioinformatic processing of the raw High-through  
354 sequence data.

355 **Figure S2.** There were significant differences across phyla among the top 10. \* and

356 \*\*\* represent statistically significant differences at  $p < 0.05$  and  $p < 0.001$  from

357 Kruskal-Wallis test. Error bars represent the means  $\pm$  SEs.

358 **Figure S3.** Venn diagram of shared and unique metabolic pathway numbers observed

359 in nano-untreated and nano-treated soil.

360 **Figure S4.** Prediction performance of Richness and Shannon using RF models. The

361 slope of the solid lines was 1, and the dotted lines represented the intercepts of  $\pm$

362 RMSE.

363

364 **References**

- 365 Ahneman, D.T., Estrada, J.G., Lin, S., Dreher, S.D., Doyle, A.G., 2018. Predicting  
366 reaction performance in C–N cross-coupling using machine learning. *Science*  
367 360, 186–190. doi:10.1126/science.aar5169
- 368 Ali, A., Guo, D., Li, Y., Shaheen, S.M., Wahid, F., Antoniadis, V., Abdelrahman, H., Al-  
369 Solaimani, S.G., Li, R., Tsang, D.C.W., Rinklebe, J., Zhang, Z., 2021.  
370 *Streptomyces pactum* addition to contaminated mining soils improved soil  
371 quality and enhanced metals phytoextraction by wheat in a green remediation  
372 trial. *Chemosphere* 273, 129692. doi:10.1016/j.chemosphere.2021.129692
- 373 Ameen, F., Alsamhary, K., Alabdullatif, J.A., ALNadhari, S., 2021. A review on metal-  
374 based nanoparticles and their toxicity to beneficial soil bacteria and fungi.  
375 *Ecotoxicology and Environmental Safety* 213, 112027.  
376 doi:10.1016/j.ecoenv.2021.112027
- 377 Asadishad, B., Chahal, S., Akbari, A., Cianciarelli, V., Azodi, M., Ghoshal, S., Tufenkji,  
378 N., 2018. Amendment of Agricultural Soil with Metal Nanoparticles: Effects on  
379 Soil Enzyme Activity and Microbial Community Composition. *Environmental*  
380 *Science & Technology* 52, 1908–1918. doi:10.1021/acs.est.7b05389
- 381 Bahram, M., Hildebrand, F., Forslund, S.K., Anderson, J.L., Soudzilovskaia, N.A.,  
382 Bodegom, P.M., Bengtsson-Palme, J., Anslan, S., Coelho, L.P., Harend, H.,  
383 Huerta-Cepas, J., Medema, M.H., Maltz, M.R., Mundra, S., Olsson, P.A., Pent,  
384 M., Pölme, S., Sunagawa, S., Ryberg, M., Tedersoo, L., Bork, P., 2018. Structure  
385 and function of the global topsoil microbiome. *Nature* 560, 233–237.

386 doi:10.1038/s41586-018-0386-6

387 Ban, Z., Yuan, P., Yu, F., Peng, T., Zhou, Q., Hu, X., 2020. Machine learning predicts  
388 the functional composition of the protein corona and the cellular recognition of  
389 nanoparticles. *Proceedings of the National Academy of Sciences* 117, 10492–  
390 10499. doi:10.1073/pnas.1919755117

391 Ban, Z., Zhou, Q., Sun, A., Mu, L., Hu, X., 2018. Screening Priority Factors  
392 Determining and Predicting the Reproductive Toxicity of Various Nanoparticles.  
393 *Environmental Science and Technology* 52, 9666–9676. doi:  
394 10.1021/acs.est.8b02757

395 Ben-Moshe, T., Frenk, S., Dror, I., Minz, D., Berkowitz, B., 2013. Effects of metal  
396 oxide nanoparticles on soil properties. *Chemosphere* 90, 640–646.  
397 doi:10.1016/j.chemosphere.2012.09.018

398 Bolyen, E., Rideout, J.R., Dillon, M.R., Bokulich, N.A., Abnet, C.C., Al-Ghalith, G.A.,  
399 Alexander, H., Alm, E.J., Arumugam, M., Asnicar, F., Bai, Y., Bisanz, J.E.,  
400 Bittinger, K., Brejnrod, A., Brislawn, C.J., Brown, C.T., Callahan, B.J.,  
401 Caraballo-Rodríguez, A.M., Chase, J., Cope, E.K., Da Silva, R., Diener, C.,  
402 Dorrestein, P.C., Douglas, G.M., Durall, D.M., Duvallet, C., Edwardson, C.F.,  
403 Ernst, M., Estaki, M., Fouquier, J., Gauglitz, J.M., Gibbons, S.M., Gibson, D.L.,  
404 Gonzalez, A., Gorlick, K., Guo, J., Hillmann, B., Holmes, S., Holste, H.,  
405 Huttenhower, C., Huttley, G.A., Janssen, S., Jarmusch, A.K., Jiang, L., Kaehler,  
406 B.D., Kang, K.B., Keefe, C.R., Keim, P., Kelley, S.T., Knights, D., Koester, I.,  
407 Kosciolk, T., Kreps, J., Langille, M.G.I., Lee, J., Ley, R., Liu, Y.-X., Loftfield,

408 E., Lozupone, C., Maher, M., Marotz, C., Martin, B.D., McDonald, D., McIver,  
409 L.J., Melnik, A.V., Metcalf, J.L., Morgan, S.C., Morton, J.T., Naimey, A.T.,  
410 Navas-Molina, J.A., Nothias, L.F., Orchanian, S.B., Pearson, T., Peoples, S.L.,  
411 Petras, D., Preuss, M.L., Pruesse, E., Rasmussen, L.B., Rivers, A., Robeson,  
412 M.S., Rosenthal, P., Segata, N., Shaffer, M., Shiffer, A., Sinha, R., Song, S.J.,  
413 Spear, J.R., Swafford, A.D., Thompson, L.R., Torres, P.J., Trinh, P., Tripathi, A.,  
414 Turnbaugh, P.J., Ul-Hasan, S., van der Hooft, J.J.J., Vargas, F., Vázquez-Baeza,  
415 Y., Vogtmann, E., von Hippel, M., Walters, W., Wan, Y., Wang, M., Warren, J.,  
416 Weber, K.C., Williamson, C.H.D., Willis, A.D., Xu, Z.Z., Zaneveld, J.R., Zhang,  
417 Y., Zhu, Q., Knight, R., Caporaso, J.G., 2019. Reproducible, interactive,  
418 scalable and extensible microbiome data science using QIIME 2. *Nature*  
419 *Biotechnology* 37, 852–857. doi:10.1038/s41587-019-0209-9

420 Callahan, B.J., McMurdie, P.J., Rosen, M.J., Han, A.W., Johnson, A.J.A., Holmes, S.P.,  
421 2016. DADA2: High-resolution sample inference from Illumina amplicon data.  
422 *Nature Methods* 13, 581–583. doi:10.1038/nmeth.3869

423 Cammarota, G., Ianiro, G., Ahern, A., Carbone, C., Temko, A., Claesson, M.J.,  
424 Gasbarrini, A., Tortora, G., 2020. Gut microbiome, big data and machine  
425 learning to promote precision medicine for cancer. *Nature Reviews*  
426 *Gastroenterology & Hepatology* 17, 635–648. doi:10.1038/s41575-020-0327-3

427 Caspi, R., Billington, R., Keseler, I.M., Kothari, A., Krummenacker, M., Midford, P.E.,  
428 Ong, W.K., Paley, S., Subhraveti, P., Karp, P.D., 2020. The MetaCyc database  
429 of metabolic pathways and enzymes - a 2019 update. *Nucleic Acids Research*

430 48, D445–D453. doi:10.1093/nar/gkz862

431 Chen, Q.-L., Zhu, D., An, X.-L., Ding, J., Zhu, Y.-G., Cui, L., 2019. Does nano silver  
432 promote the selection of antibiotic resistance genes in soil and plant?  
433 Environment International 128, 399–406. doi:10.1016/j.envint.2019.04.061

434 Coccozza, C., Perone, A., Giordano, C., Salvatici, M.C., Pignattelli, S., Raio, A., Schaub,  
435 M., Sever, K., Innes, J.L., Tognetti, R., Cherubini, P., 2019. Silver nanoparticles  
436 enter the tree stem faster through leaves than through roots. Tree Physiology 39,  
437 1251–1261. doi:10.1093/treephys/tpz046

438 Delgado-Baquerizo, M., Maestre, F.T., Reich, P.B., Jeffries, T.C., Gaitan, J.J., Encinar,  
439 D., Berdugo, M., Campbell, C.D., Singh, B.K., 2016. Microbial diversity drives  
440 multifunctionality in terrestrial ecosystems. Nature Communications 7, 10541.  
441 doi:10.1038/ncomms10541

442 Douglas, G.M., Maffei, V.J., Zaneveld, J.R., Yurgel, S.N., Brown, J.R., Taylor, C.M.,  
443 Huttenhower, C., Langille, M.G.I., 2020. PICRUSt2 for prediction of  
444 metagenome functions. Nature Biotechnology 38, 685–688.  
445 doi:10.1038/s41587-020-0548-6

446 Fan, X., Xu, J., Lavoie, M., Peijnenburg, W.J.G.M., Zhu, Y., Lu, T., Fu, Z., Zhu, T.,  
447 Qian, H., 2018. Multiwall carbon nanotubes modulate paraquat toxicity in  
448 Arabidopsis thaliana. Environmental Pollution 233, 633–641.  
449 doi:10.1016/j.envpol.2017.10.116

450 Fang, H., Han, L., Zhang, H., Long, Z., Cai, L., Yu, Y., 2018. Dissemination of antibiotic  
451 resistance genes and human pathogenic bacteria from a pig feedlot to the



452 surrounding stream and agricultural soils. *Journal of Hazardous Materials* 357,  
453 53–62. doi:10.1016/j.jhazmat.2018.05.066

454 Fayaz, A.M., Balaji, K., Girilal, M., Kalaichelvan, P.T., Venkatesan, R., 2009.  
455 Mycobased Synthesis of Silver Nanoparticles and Their Incorporation into  
456 Sodium Alginate Films for Vegetable and Fruit Preservation. *Journal of*  
457 *Agricultural and Food Chemistry* 57, 6246–6252. doi:10.1021/jf900337h

458 Finkel, O.M., Salas-González, I., Castrillo, G., Conway, J.M., Law, T.F., Teixeira,  
459 P.J.P.L., Wilson, E.D., Fitzpatrick, C.R., Jones, C.D., Dangl, J.L., 2020. A single  
460 bacterial genus maintains root growth in a complex microbiome. *Nature* 587,  
461 103–108. doi:10.1038/s41586-020-2778-7

462 Guerriero, G., Sutura, F.M., Torabi-Pour, N., Renaut, J., Hausman, J.-F., Berni, R.,  
463 Pennington, H.C., Welsh, M., Dehsorkhi, A., Zancan, L.R., Saffie-Siebert, S.,  
464 2021. Phyto-Courier, a Silicon Particle-Based Nano-biostimulant: Evidence  
465 from *Cannabis sativa* Exposed to Salinity. *ACS Nano* 15, 3061–3069.  
466 doi:10.1021/acsnano.0c09488

467 Guo, Z., Wan, S., Hua, K., Yin, Y., Chu, H., Wang, D., Guo, X., 2020. Fertilization  
468 regime has a greater effect on soil microbial community structure than crop  
469 rotation and growth stage in an agroecosystem. *Applied Soil Ecology* 149,  
470 103510. doi:10.1016/j.apsoil.2020.103510

471 Hendren, C.O., Mesnard, X., Dröge, J., Wiesner, M.R., 2011. Estimating Production  
472 Data for Five Engineered Nanomaterials As a Basis for Exposure Assessment.  
473 *Environmental Science & Technology* 45, 2562–2569. doi:10.1021/es103300g

474 Hibbing, M.E., Fuqua, C., Parsek, M.R., Peterson, S.B., 2010. Bacterial competition:  
475 surviving and thriving in the microbial jungle. *Nature Reviews Microbiology* 8,  
476 15–25. doi:10.1038/nrmicro2259

477 Jordan, M.I., Mitchell, T.M., 2015. Machine learning: Trends, perspectives, and  
478 prospects. *Science* 349, 255–260. doi:10.1126/science.aaa8415

479 Ke, M., Li, Y.,  
480 Qu, Q., Ye, Y., Peijnenburg, W.J.G.M., Zhang, Z., Xu, N., Lu, T., Sun, L., Qian,  
481 H., 2020. Offspring toxicity of silver nanoparticles to *Arabidopsis thaliana*  
482 flowering and floral development. *Journal of Hazardous Materials* 386, 121975.  
doi:10.1016/j.jhazmat.2019.121975

483 Ke, M., Ye, Y., Zhang, Z., Gillings, M., Qu, Q., Xu, N., Xu, L., Lu, T., Wang, J., Qian,  
484 H., 2021. Synergistic effects of glyphosate and multiwall carbon nanotubes on  
485 *Arabidopsis thaliana* physiology and metabolism. *Science of The Total*  
486 *Environment* 769, 145156. doi:10.1016/j.scitotenv.2021.145156

487 Kusi, J., Scheuerman, P.R., Maier, K.J., 2020. Emerging environmental contaminants  
488 (silver nanoparticles) altered the catabolic capability and metabolic  
489 fingerprinting of microbial communities. *Aquatic Toxicology* 228, 105633.  
490 doi:10.1016/j.aquatox.2020.105633

491 Kielak, A.M., Veen, J.A. van., Kowalchuk,  
492 G.A., 2010. Comparative Analysis of Acidobacterial Genomic Fragments from  
493 Terrestrial and Aquatic Metagenomic Libraries, with Emphasis on  
494 Acidobacteria Subdivision 6. *Applied and Environmental Microbiology* 76,  
6769–6777. doi:10.1128/AEM.00343-10

495 Lehmann, A., Zheng, W. Rillig, M.C. Soil biota contributions to soil aggregation.

496 Nature Ecology and Evolution 1, 1828–1835. doi:10.1038/s41559-017-0344-y

497 Martin, M., 2011. Cutadapt removes adapter sequences from high-throughput  
498 sequencing reads. EMBnet.Journal. doi:10.14806/ej.17.1.200

499 McShane, H., Sarrazin, M., Whalen, J.K., Hendershot, W.H., Sunahara, G.I., 2012.  
500 Reproductive and behavioral responses of earthworms exposed to nano-sized  
501 titanium dioxide in soil. Environmental Toxicology and Chemistry 31, 184–193.  
502 doi:10.1002/etc.714

503 Moll, J., Klingenfuss, F., Widmer, F., Gogos, A., Bucheli, T.D., Hartmann, M., van der  
504 Heijden, M.G.A., 2017. Effects of titanium dioxide nanoparticles on soil  
505 microbial communities and wheat biomass. Soil Biology and Biochemistry 111,  
506 85–93. doi:10.1016/j.soilbio.2017.03.019

507 Montes de Oca-Vásquez, G., Solano-Campos, F., Vega-Baudrit, J.R., López-Mondéjar,  
508 R., Vera, A., Moreno, J.L., Bastida, F., 2020. Organic amendments exacerbate  
509 the effects of silver nanoparticles on microbial biomass and community  
510 composition of a semiarid soil. Science of The Total Environment 744, 140919.  
511 doi:10.1016/j.scitotenv.2020.140919

512 Nilsson, R.H., Anslan, S., Bahram, M., Wurzbacher, C., Baldrian, P., Tedersoo, L., 2019.  
513 Mycobiome diversity: high-throughput sequencing and identification of fungi.  
514 Nature Reviews Microbiology 17, 95–109. doi:10.1038/s41579-018-0116-y

515 Oh, E., Liu, R., Nel, A., Gemill, K.B., Bilal, M., Cohen, Y., Medintz, I.L., 2016. Meta-  
516 analysis of cellular toxicity for cadmium-containing quantum dots. Nature  
517 Nanotechnology 11, 479–486. doi:10.1038/nnano.2015.338

518 Peng, C., Xu, C., Liu, Q., Sun, L., Luo, Y., Shi, J., 2017. Fate and Transformation of  
519 CuO Nanoparticles in the Soil–Rice System during the Life Cycle of Rice  
520 Plants. *Environmental Science & Technology* 51, 4907–4917.  
521 doi:10.1021/acs.est.6b05882

522 Qu, Q., Zhang, Z., Peijnenburg, W.J.G.M., Liu, W., Lu, T., Hu, B., Chen, Jianmeng,  
523 Chen, Jun, Lin, Z., Qian, H., 2020. Rhizosphere Microbiome Assembly and Its  
524 Impact on Plant Growth. *Journal of Agricultural and Food Chemistry* 68, 5024–  
525 5038. doi:10.1021/acs.jafc.0c00073

526 Rajput, V.D., Minkina, T.M., Behal, A., Sushkova, S.N., Mandzhieva, S., Singh, R.,  
527 Gorovtsov, A., Tsitsuashvili, V.S., Purvis, W.O., Ghazaryan, K.A., Movsesyan,  
528 H.S., 2018. Effects of zinc-oxide nanoparticles on soil, plants, animals and soil  
529 organisms: A review. *Environmental Nanotechnology, Monitoring &*  
530 *Management* 9, 76–84. doi:10.1016/j.enmm.2017.12.006

531 Ramirez, K.S., Knight, C.G., de Hollander, M., Brearley, F.Q., Constantinides, B.,  
532 Cotton, A., Creer, S., Crowther, T.W., Davison, J., Delgado-Baquerizo, M.,  
533 Dorrepaal, E., Elliott, D.R., Fox, G., Griffiths, R.I., Hale, C., Hartman, K.,  
534 Houlden, A., Jones, D.L., Krab, E.J., Maestre, F.T., McGuire, K.L., Monteux,  
535 S., Orr, C.H., van der Putten, W.H., Roberts, I.S., Robinson, D.A., Rocca, J.D.,  
536 Rowntree, J., Schlaeppli, K., Shepherd, M., Singh, B.K., Straathof, A.L.,  
537 Bhatnagar, J.M., Thion, C., van der Heijden, M.G.A., de Vries, F.T., 2018.  
538 Detecting macroecological patterns in bacterial communities across  
539 independent studies of global soils. *Nature Microbiology* 3, 189–196.

540           doi:10.1038/s41564-017-0062-x

541   Ranjard, L., Dequiedt, S., Prévost-Bouré, N. C., Thioulouse, J., Saby, N.P.A., Lelievre,  
542           M., Maron, P.A., Morin, F.E.R., Bispo, A., Jolivet, C., Arrouays, D., Lemanceau,  
543           P., 2013. Turnover of soil bacterial diversity driven by wide-scale environmental  
544           heterogeneity. *Nature Communications* 4, 1434. doi:10.1038/ncomms2431

545   Ray, P., Lakshmanan, V., Labbé, J.L., Craven, K.D., 2020. Microbe to Microbiome: A  
546           Paradigm Shift in the Application of Microorganisms for Sustainable  
547           Agriculture. *Frontiers in Microbiology* 11. doi:10.3389/fmicb.2020.622926

548   Shin, N.-R., Whon, T.W., Bae, J.-W., 2015. Proteobacteria: microbial signature of  
549           dysbiosis in gut microbiota. *Trends in Biotechnology* 33, 496–503.  
550           doi:10.1016/j.tibtech.2015.06.011

551   Simonin, M., Cantarel, A.A.M., Crouzet, A., Gervaix, J., Martins, J.M.F., Richaume,  
552           A., 2018. Negative effects of copper oxide nanoparticles on carbon and nitrogen  
553           cycle microbial activities in contrasting agricultural soils and in presence of  
554           plants. *Frontiers in Microbiology* 9, 3102-3102. doi:10.3389/fmicb.2018.03102

555   Simonin, M., Richaume, A., 2015. Impact of engineered nanoparticles on the activity,  
556           abundance, and diversity of soil microbial communities: a review.  
557           *Environmental Science and Pollution Research* 22, 13710–13723.  
558           doi:10.1007/s11356-015-4171-x

559   Sun, T., Conroy, G., Donner, E., Hungerbuhler,  
560           K., Lombi, E., Nowack, B., 2015. Probabilistic modelling of engineered  
561           nanomaterial emissions to the environment: a spatio-temporal approach 2, 340-  
          351. doi:10.1039/c5en00004a

562 Tapia-García, E.Y., Hernández-Trejo, V., Guevara-Luna, J., Rojas-Rojas, F.U., Arroyo-  
563 Herrera, I., Meza-Radilla, G., Vásquez-Murrieta, M.S., Estrada-de los Santos,  
564 P., 2020. Plant growth-promoting bacteria isolated from wild legume nodules  
565 and nodules of *Phaseolus vulgaris* L. trap plants in central and southern Mexico.  
566 *Microbiological Research* 239, 126522. doi:10.1016/j.micres.2020.126522

567 Tian, L., Shen, J., Sun, G., Wang, B., Ji, R., Zhao, L., 2020. Foliar Application of SiO<sub>2</sub>  
568 Nanoparticles Alters Soil Metabolite Profiles and Microbial Community  
569 Composition in the Pakchoi (*Brassica chinensis* L.) Rhizosphere Grown in  
570 Contaminated Mine Soil. *Environmental Science & Technology* 54, 13137–  
571 13146. doi:10.1021/acs.est.0c03767

572 Wang, X., Cui, Y., Zhang, X., Ju, W., Duan, C., Wang, Y., Fang, L., 2020. A novel  
573 extracellular enzyme stoichiometry method to evaluate soil heavy metal  
574 contamination: Evidence derived from microbial metabolic limitation. *Science*  
575 *of The Total Environment* 738, 139709. doi:10.1016/j.scitotenv.2020.139709

576 Wiegand, S., Jogler, M., Jogler, C., 2018. On the maverick Planctomycetes. *FEMS*  
577 *Microbiology Reviews* 42, 739–760. doi:10.1093/femsre/fuy029

578 Wright, R.J., Langille, M.G.I., Walker, T.R., 2021. Food or just a free ride? A meta-  
579 analysis reveals the global diversity of the Plastisphere. *The ISME Journal* 15,  
580 789–806. doi:10.1038/s41396-020-00814-9

581 Yang, L., Barnard, R., Kuzyakov, Y., Tian, J., 2021. Bacterial communities drive the  
582 resistance of soil multifunctionality to land-use change in karst soils. *European*  
583 *Journal of Soil Biology* 104, 103313. doi:10.1016/j.ejsobi.2021.103313

584 Yang, Y., Rossel, R.A.V., Li, S., Bissett, A., Lee, J., Shi, Z., Behrens, T., Court, L., 2019.  
585 Soil bacterial abundance and diversity better explained and predicted with  
586 spectro-transfer functions. *Soil Biology and Biochemistry* 129, 29–  
587 38. doi:10.1016/j.soilbio.2018.11.005

588 You, T., Liu, D., Chen, J., Yang, Z., Dou, R., Gao, X., Wang, L., 2018. Effects of metal  
589 oxide nanoparticles on soil enzyme activities and bacterial communities in two  
590 different soil types. *Journal of Soils and Sediments* 18, 211–221.  
591 doi:10.1007/s11368-017-1716-2

592 You, X., Suo, F., Yin, S., Wang, X., Zheng, H., Fang, S., Zhang, C., Li, F., Li, Y., 2021.  
593 Biochar decreased enantioselective uptake of chiral pesticide metalaxyl by  
594 lettuce and shifted bacterial community in agricultural soil. *Journal of*  
595 *Hazardous Materials* 417, 126047. doi:10.1016/j.jhazmat.2021.126047

596 Yu, F., Wei, C., Deng, P., Peng, T., Hu, X., 2021. Deep exploration of random forest  
597 model boosts the interpretability of machine learning studies of complicated  
598 immune responses and lung burden of nanoparticles. *Science Advances* 7,  
599 eabf4130. doi:10.1126/sciadv.abf4130

600 Yuan, J., Wen, T., Zhang, H., Zhao, M., Penton, C.R., Thomashow, L.S., Shen, Q., 2020.  
601 Predicting disease occurrence with high accuracy based on soil macroecological  
602 patterns of *Fusarium* wilt. *The ISME Journal* 14, 2936–2950.  
603 doi:10.1038/s41396-020-0720-5

604 Zhang, H., Huang, M., Zhang, W., Gardea-Torresdey, J.L., White, J.C., Ji, R., Zhao, L.,  
605 2020a. Silver Nanoparticles Alter Soil Microbial Community Compositions and

606 Metabolite Profiles in Unplanted and Cucumber-Planted Soils. *Environmental*  
607 *Science & Technology* 54, 3334–3342. doi:10.1021/acs.est.9b07562

608 Zhang, P., Guo, Z., Zhang, Z., Fu, H., White, J.C., Lynch, I., 2020b. Nanomaterial  
609 Transformation in the Soil–Plant System: Implications for Food Safety and  
610 Application in Agriculture. *Small* 16, doi:10.1002/sml.202000705

611 Zhang, Z., Ke, M., Qu, Q., Peijnenburg, W.J.G.M., Lu, T., Zhang, Q., Ye, Y., Xu, P., Du,  
612 B., Sun, L., Qian, H., 2018. Impact of copper nanoparticles and ionic copper  
613 exposure on wheat (*Triticum aestivum* L.) root morphology and antioxidant  
614 response. *Environmental Pollution* 239, 689–697.  
615 doi:10.1016/j.envpol.2018.04.066

616 Zhou, Z., Wang, C., Jiang, L., Luo, Y., 2017. Trends in soil microbial communities  
617 during secondary succession. *Soil Biology and Biochemistry* 115, 92–99.  
618 doi:10.1016/j.soilbio.2017.08.014

619

620



621 **Figure legends**

622 **Figure 1** Overview of sample collection. The geographic region information about  
623 sampling sites, and the number of independent studies and samples in this study were  
624 displayed. A dot represents a single independent experiment.

625 **Figure 2** Effects of the NPs on diversity and structure of microbial communities.

626 (a) Alpha diversity of soil bacterial community. The Shannon and Richness indices  
627 were calculated with all amplicon sequence variants (ASVs) merged from 365  
628 samples. (b) Principal coordinates analysis (PCoA) with Bray–Curtis dissimilarity  
629 performed on the taxonomic (at the genus level) for nano-untreated and nano-treated  
630 group. Statistical significance was evaluated via PERMANOVA test. (c) Relative  
631 abundance of the 10 most abundant phyla in nano-untreated and nano-treated group.  
632 (d) Venn diagram of shared and unique genus numbers observed in nano-untreated  
633 and nano-treated soil.

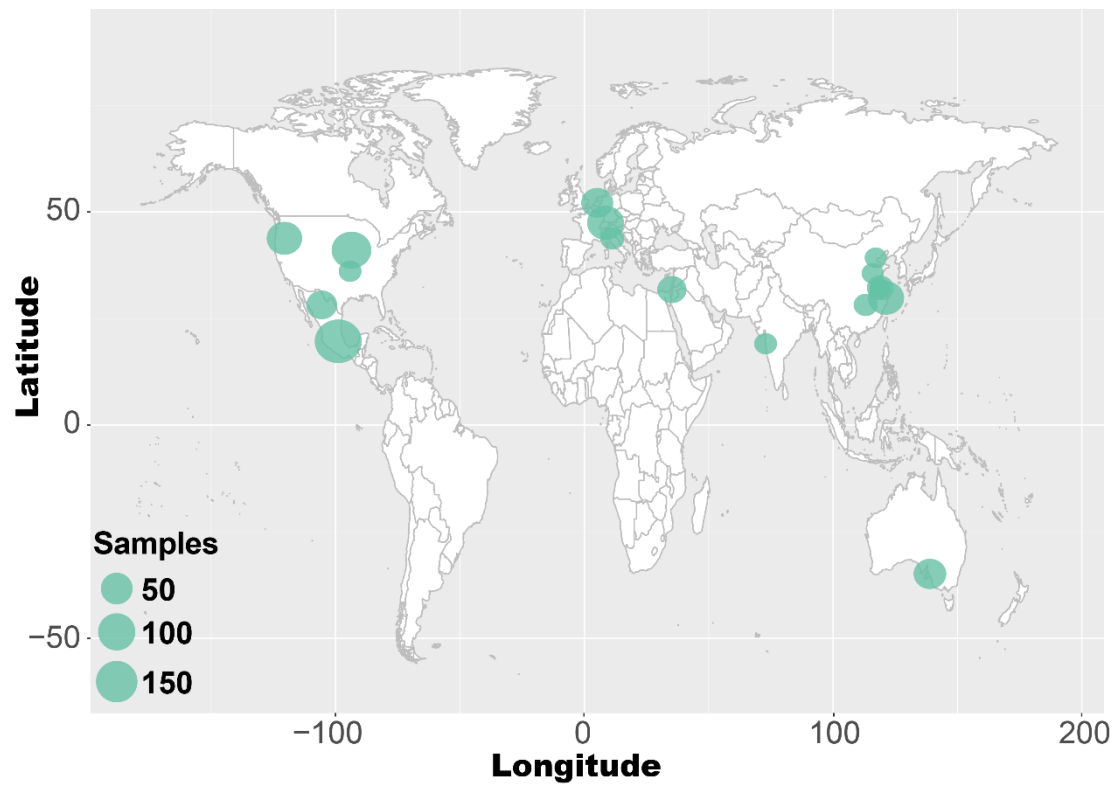
634 **Figure 3** Profile of beneficial and pathogenic soil bacteria following treatment of  
635 NPs'. (a), (b), (c) and (d) Differentially beneficial bacteria at genus level after NPs  
636 treatment. (e) Differentially pathogenic bacterium at genus level after NPs treatment.  
637 The significant difference evaluated by Kruskal-Wallis test ( $p < 0.05$ ).

638 **Figure 4** Functional pathways of the microbial communities altered after NPs  
639 treatment. The different colors of the outermost layer represented different categories  
640 of metabolic pathway functions. The inner circles represented the functional pathways  
641 at BioCyc ID level. Pathways showing significant difference ( $p < 0.05$ ) between the  
642 nano-untreated and nano-treated group are colored according to direction of change

643 by treatment. The size of circles represented the change-fold of the functional  
644 pathway abundance after NPs treatment. The change-fold represented the ratio of  
645 nano-treated to nano-untreated functional pathways.

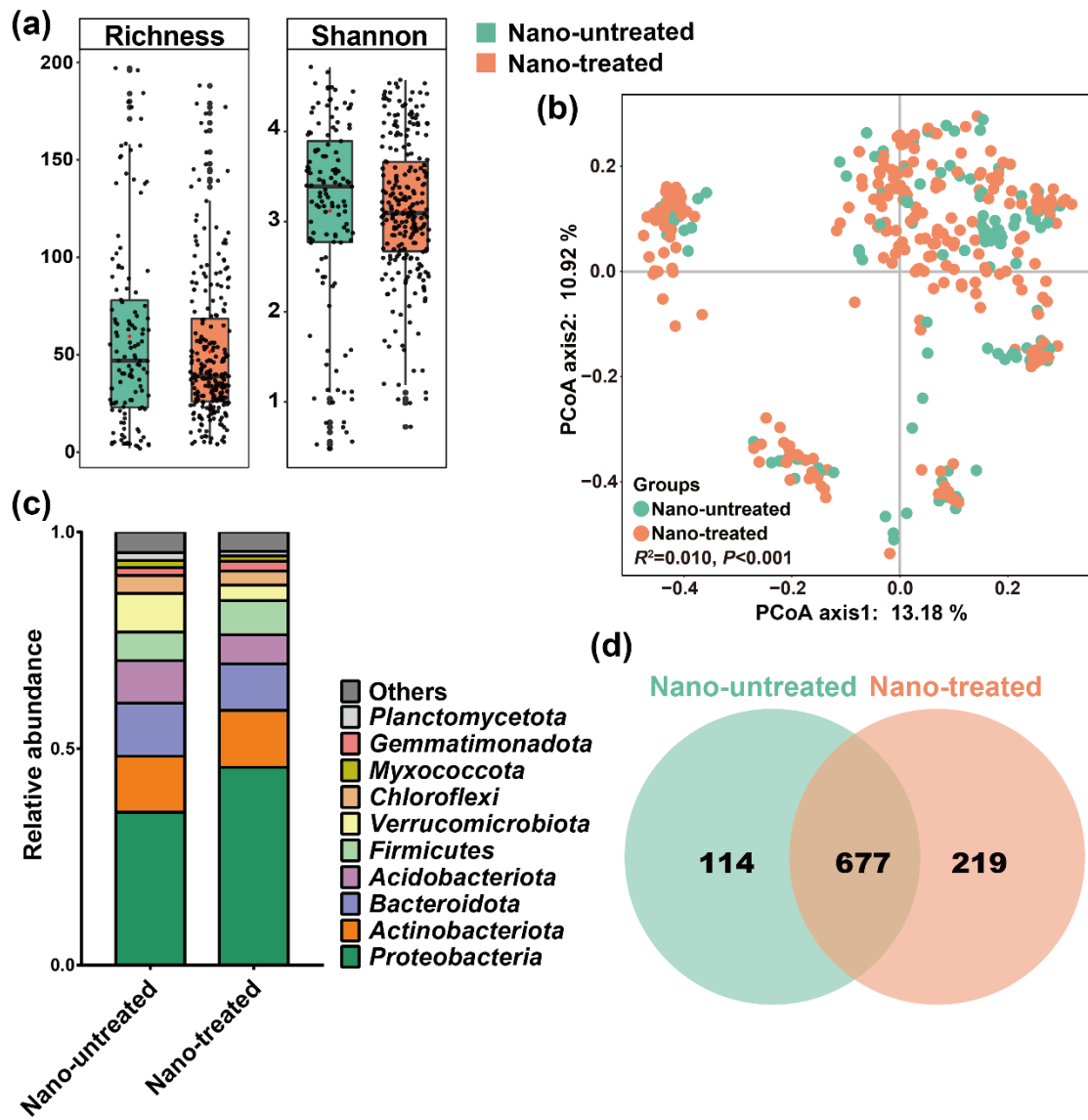
646 **Figure 5** Model building by Random Forest for connection between NPs  
647 characteristics and microbial community traits. (a) The values of  $R^2$  in validation  
648 model evaluated by tenfold cross-validation. (b) and (c) The contribution of NPs  
649 characteristics of Richness and Shannon models on microbial traits. Orange  
650 represented the heterogeneity factors, and green represented the NPs factors. The  
651 larger the arc of the circle, the more important the factors. The letter abbreviations  
652 represent the following: A, Bulk group; B, NPs type; C, NPs category; D, Dispersion  
653 medium; E, NPs existence state; F, NPs shape; G, NPs size; H, Zeta potential; I,  
654 Dispersion medium pH; J, Exposure time; K, Temperature; L, Extent of  
655 agglomeration; M, Crystal structure; N, NPs concentration; O, Soil type; P,  
656 Rhizosphere microbiota; Q, Soil pH; R, Soil depth; S, Longitude; T, Latitude; X,  
657 Amplicon area. (d) Correlation analysis of the most important NPs factor and  
658 microbial diversity. The green dots indicate the changefold of Richness, and the  
659 yellow dots mean the changefold of Shannon. (e) Correlation analysis of the most  
660 important NPs factor and beneficial and pathogenic bacteria. The green dots indicate  
661 the changefold of beneficial bacteria, and the yellow dots mean the changefold of  
662 pathogenic bacterium. The shapes of the dots represent different bacteria. The  
663 changefold represents the ratio of the value of nano-treated to nano-untreated.

664 **Figure 1**

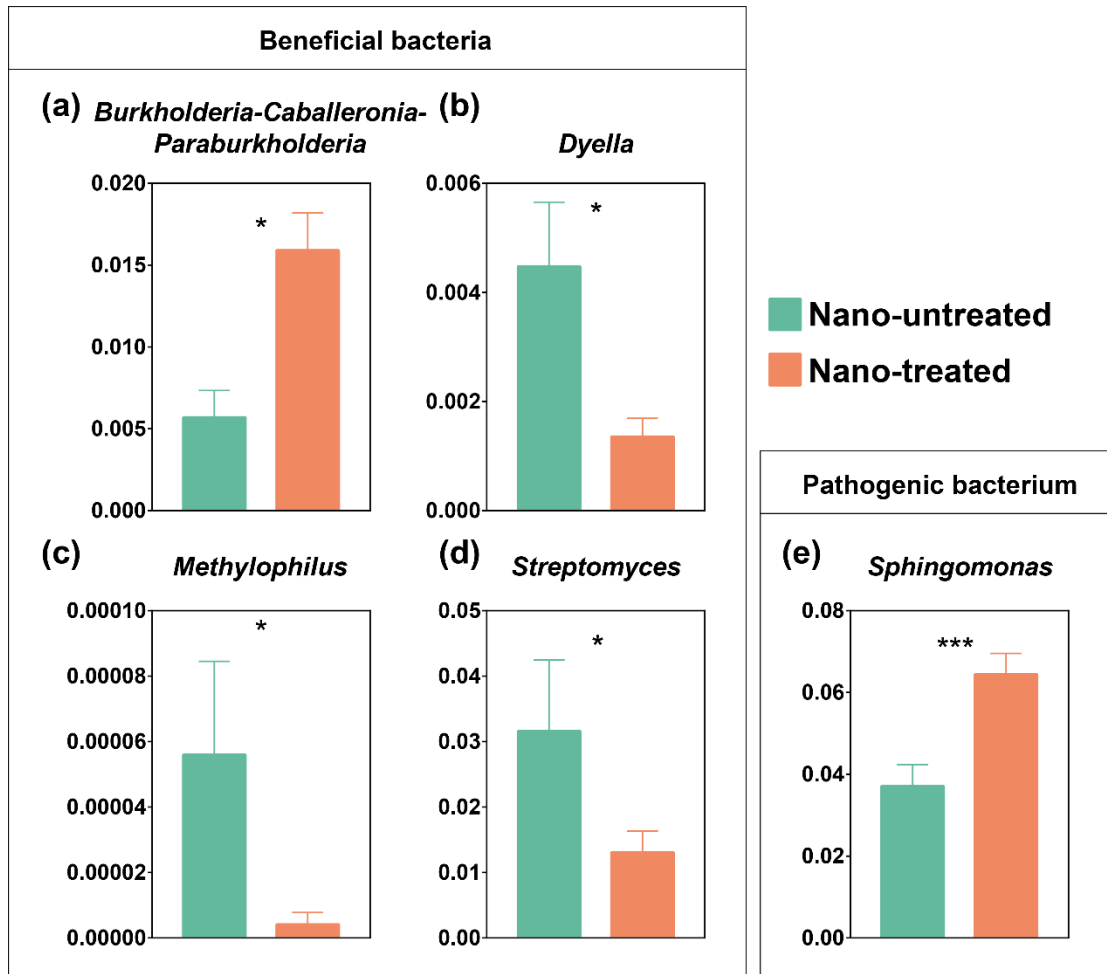


665

666

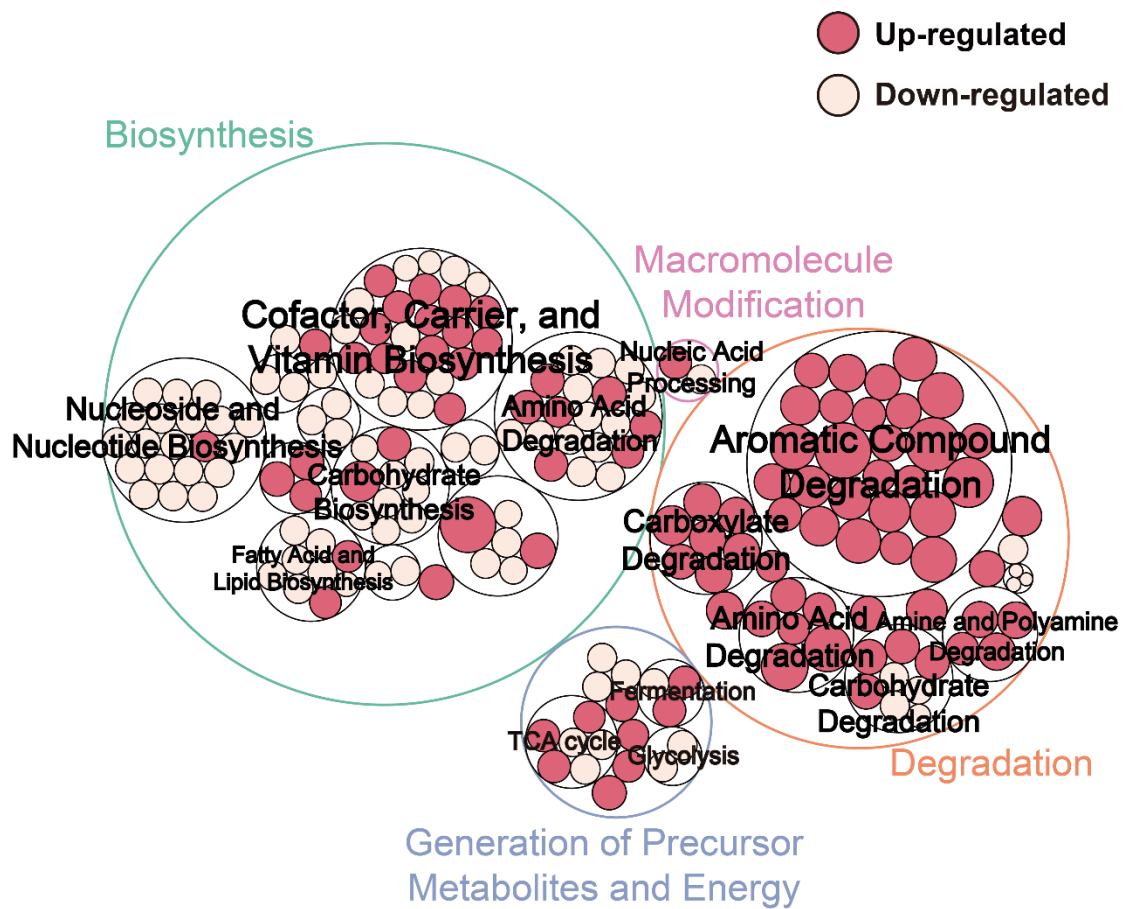


670 **Figure 3**



671

672



674

675

